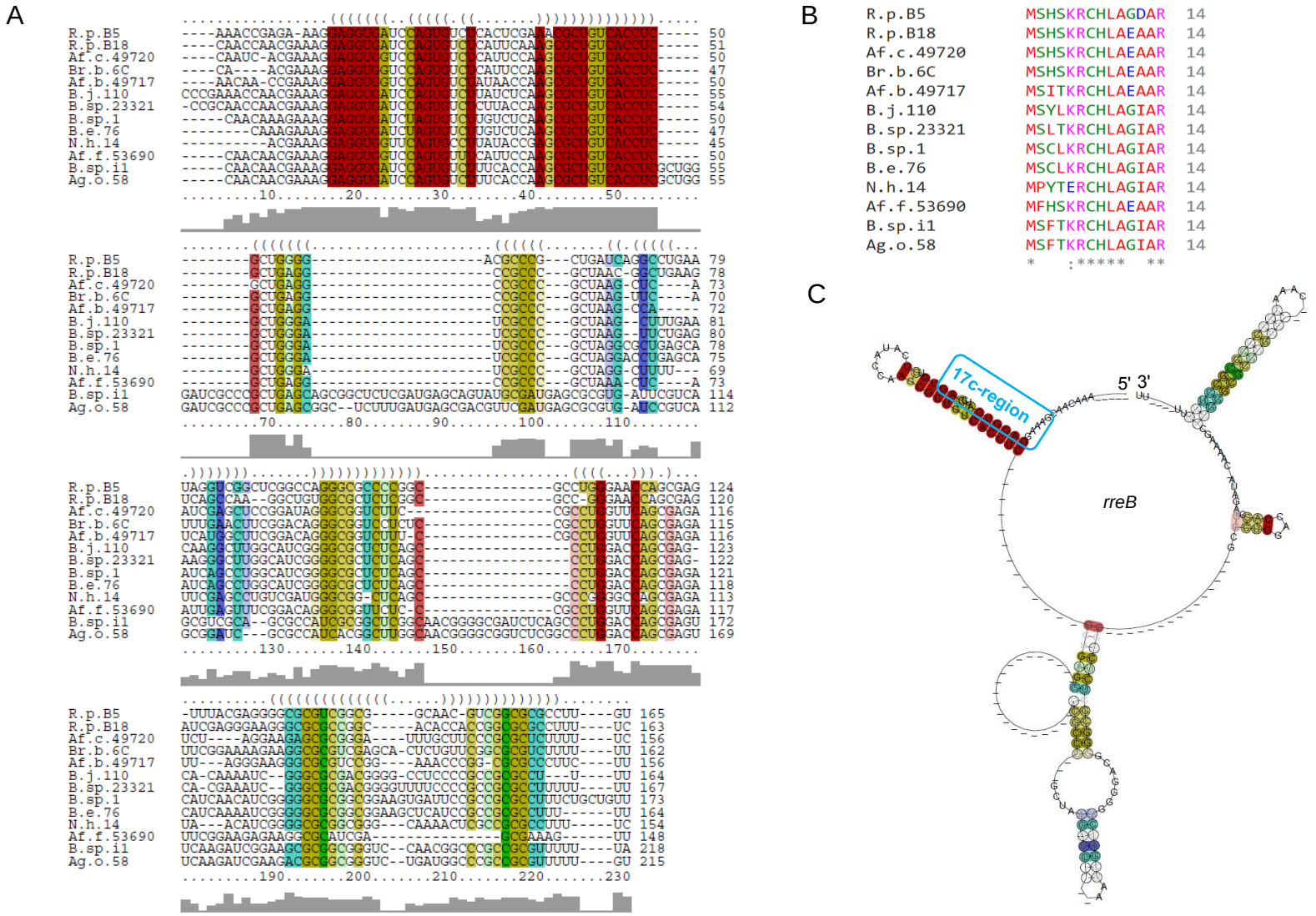

Figure S1 Conservation of *rreB* in *Bradyrhizobiaceae*. A) LocARNA alignment of RNA sequences with homology to *rreB*. The LocARNA color annotation shows the conservation of base pairs (Smith et al, 2010)**.** R.p.B5, *Rhodopseudomonas palustris* BisB5 (HaA2); R.p.B18, *R. palustrus* BisB18; Af.c.49720, *Afipia clevelandensis* ATCC 49720; Br.b.6C, *Bradyrhizobiaceae bacterium* SG6C; Af. b.49717, *Afipia broomeae* ATCC 49717; B. j.110, *B. japonicum* USDA 110; B.sp.23321, *Bradyrhizobium sp.* S23321; B. sp.1, *Bradyrhizobium japonicum* strain E109 (USDA6); B.e.76, *Bradyrhizobium elkanii* USDA 76; N.h.14, *Nitrobacter hamburgensis* X14; Af.f.53690, *Afipia felis* ATCC 53690; B. sp i1, *Bradyrhizobium sp.* BTAi1; Ag.o.58, *Agromonas oligotrophica* (*Bradyrhizobium oligotrophicum*) S58. **B)** Clustal O(1.2.3) multiple sequence alignment of the small proteins encoded by *rreB* and its homologs shown in A). **C)** Predicted RNA secondary structure of the *rreB* homologs shown in A). The LocARNA color annotation shows the conservation of base pairs. Highly conserved base pairs are in red. The sharpness of the appearance of nucleotides in the secondary structure is reflected by their conservation (compare to panel A).

References:

Smith C, Heyne S, Richter AS, Will S, Backofen R. Freiburg RNA Tools: a web server integrating INTARNA, EXPARNA and LOCARNA. Nucleic Acids Res 2010; 38(Web Server issue):W373-7.

Larkin MA, Blackshields G, Brown NP, Chenna R, McGettigan PA, McWilliam H, Valentin F, Wallace IM, Wilm A, Lopez R, Thompson JD, Gibson TJ, Higgins DG. (2007). Clustal W and Clustal X version 2.0. *Bioinformatics*, 23, 2947-2948.

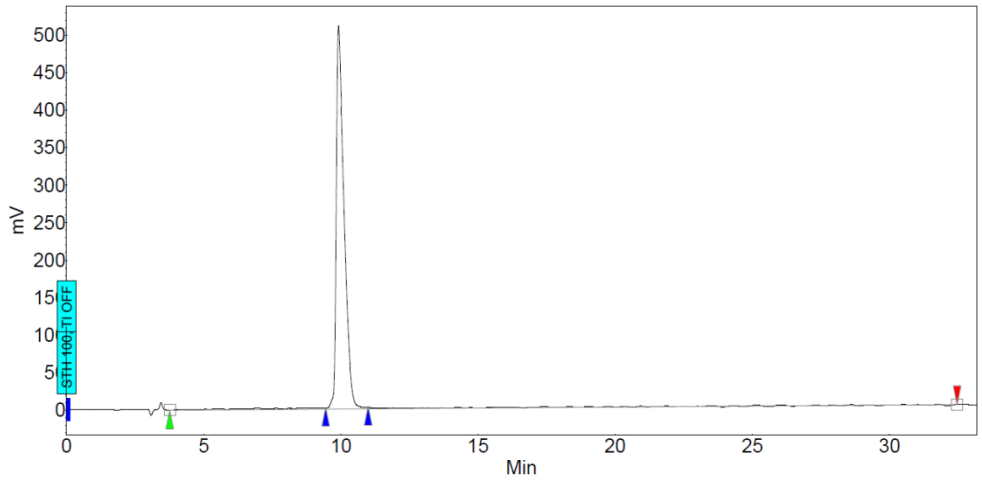

Figure S2: analytical HPLC-chromatogram of the purified RreB. The purity was >95%.

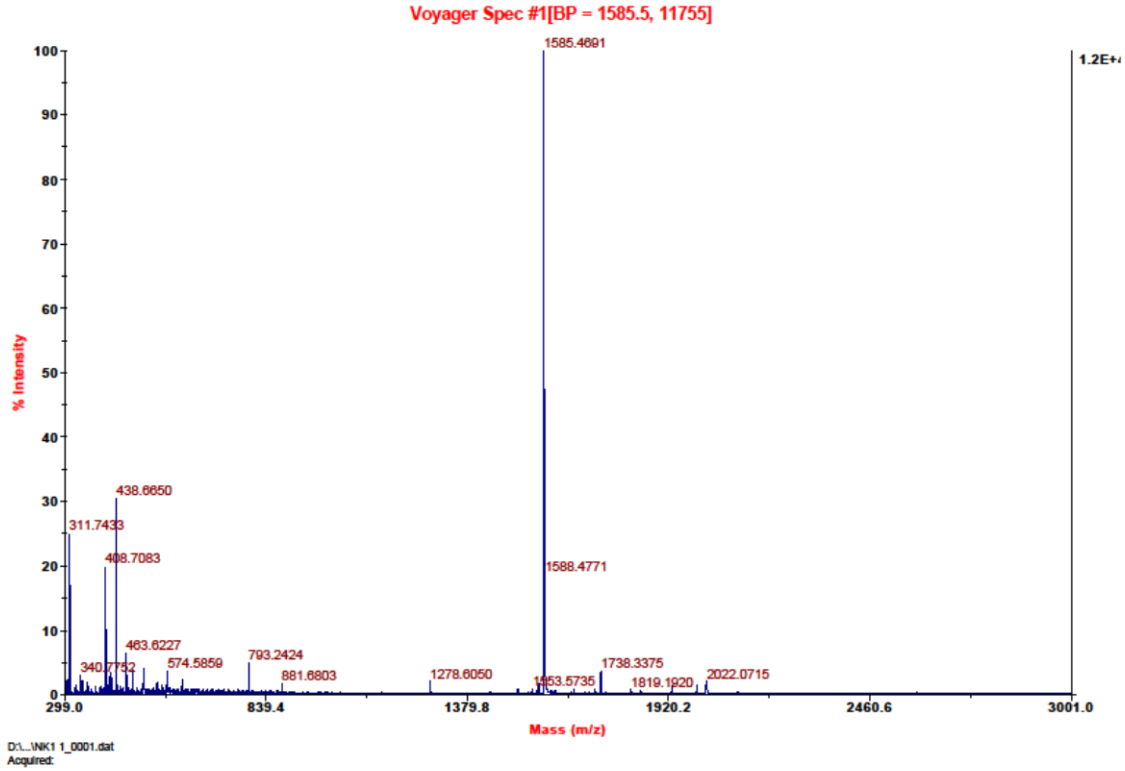

Figure S3: Matrix-assisted laser desorption/Ionization (MALDI) mass analysis of the purified RreB.

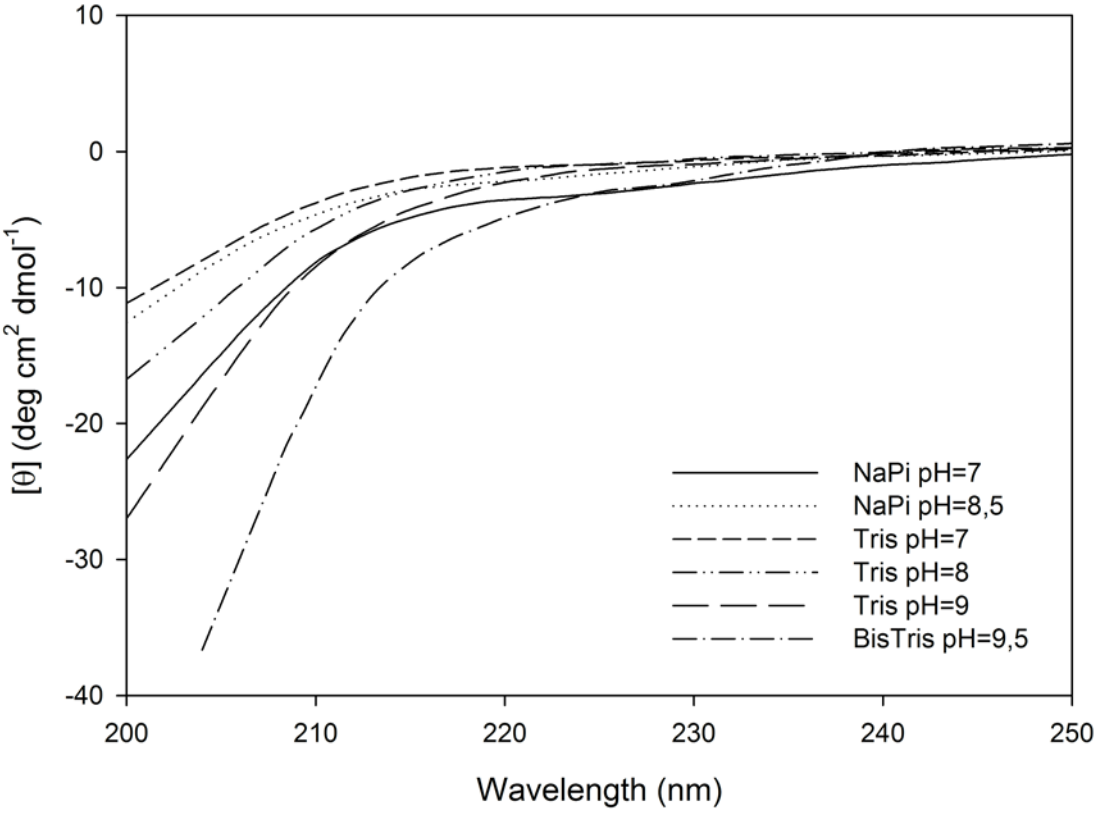

Figure S4: CD-spectra of RreB in different buffers.

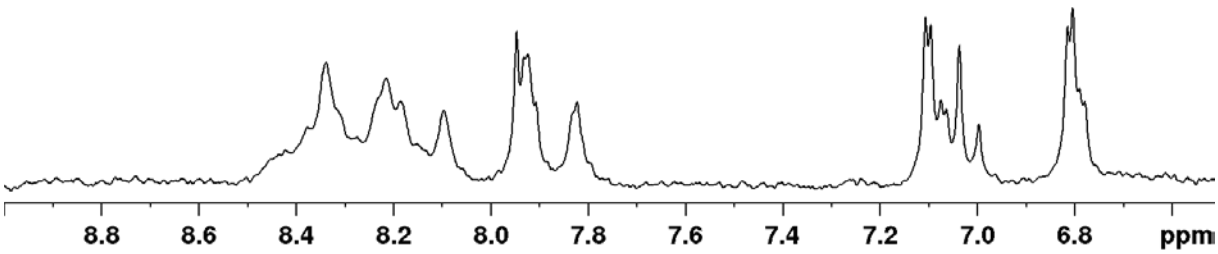

Figure S5: 1D ^{1}H-NMR-spectra of the amide, amino and aromatic proton resonances of RreB.

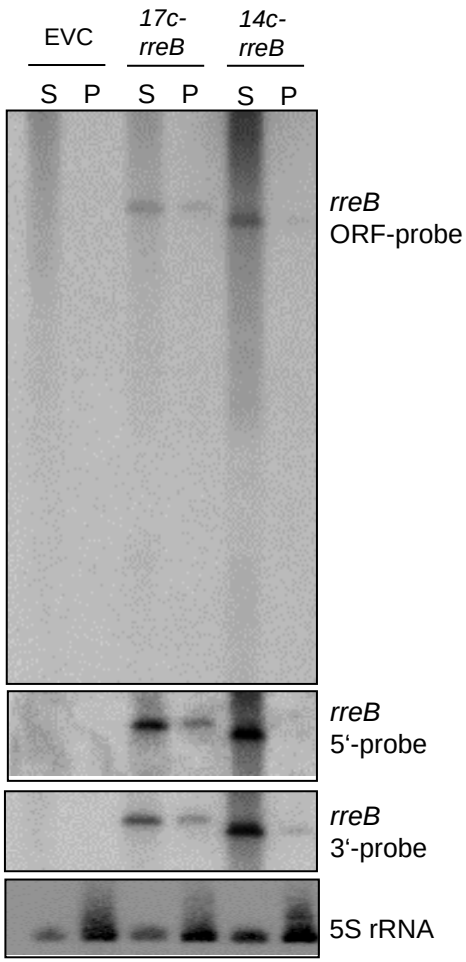

Figure S6. Distribution of *rreB*-derivatives in S100 (S) and P100 (P) fractions in *E. coli*. Northern blot analysis with the indicated probes. For schematic representation of 17c-rreB and 14c-rreB see Fig. 4 in the main text. The oligonucleotide probes are given in Table S2.

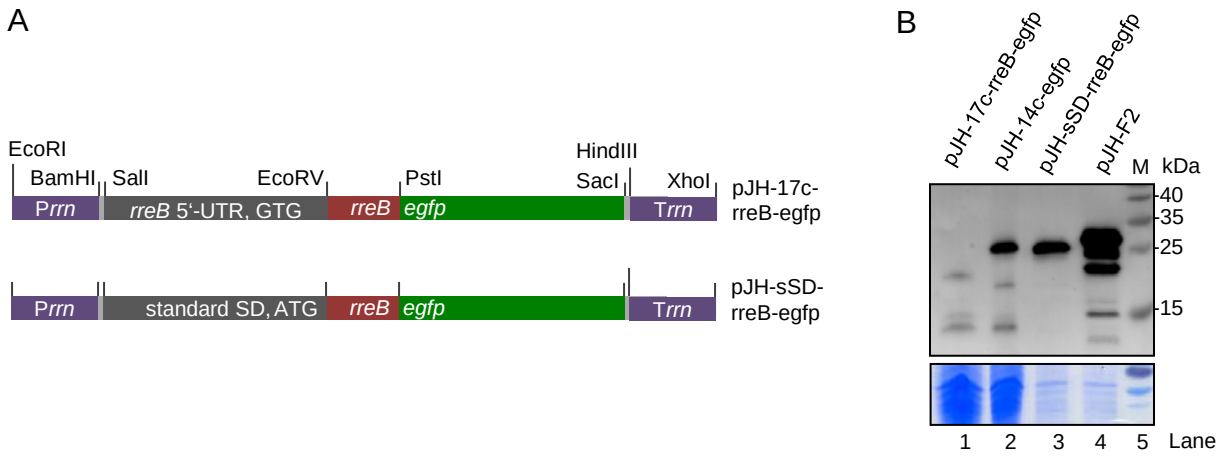

Figure S7. The *rreB-egfp* fusion preceded by full-length *rreB* 5'-UTR seems to be translated in *B. japonicum*. **A)** Schematic representation of the used constructs. The *rreB*:-*egfp* fusion is preceded either by a standard SD and an ATG start codon (standard RBS; pJH-sSD-rreB-egfp) or by the full-length 5'-UTR of *rreB* with the 17c-region and a GTG start codon (pJH-17c-rreB-egfp). **B)** Western blot analysis using EGFP-specific antibodies of strains containing the constructs shown in A). Strains with pJH-14c-egfp and pJH-F2 (see Fig. 5) were used as controls. The bottom panel shows a Coomassie Blue stained SDS-polyacrylamide gels after electrophoresis visualizing the loaded protein amounts. Migration of marker proteins (M) in the gel is indicated at the right side in kDa.

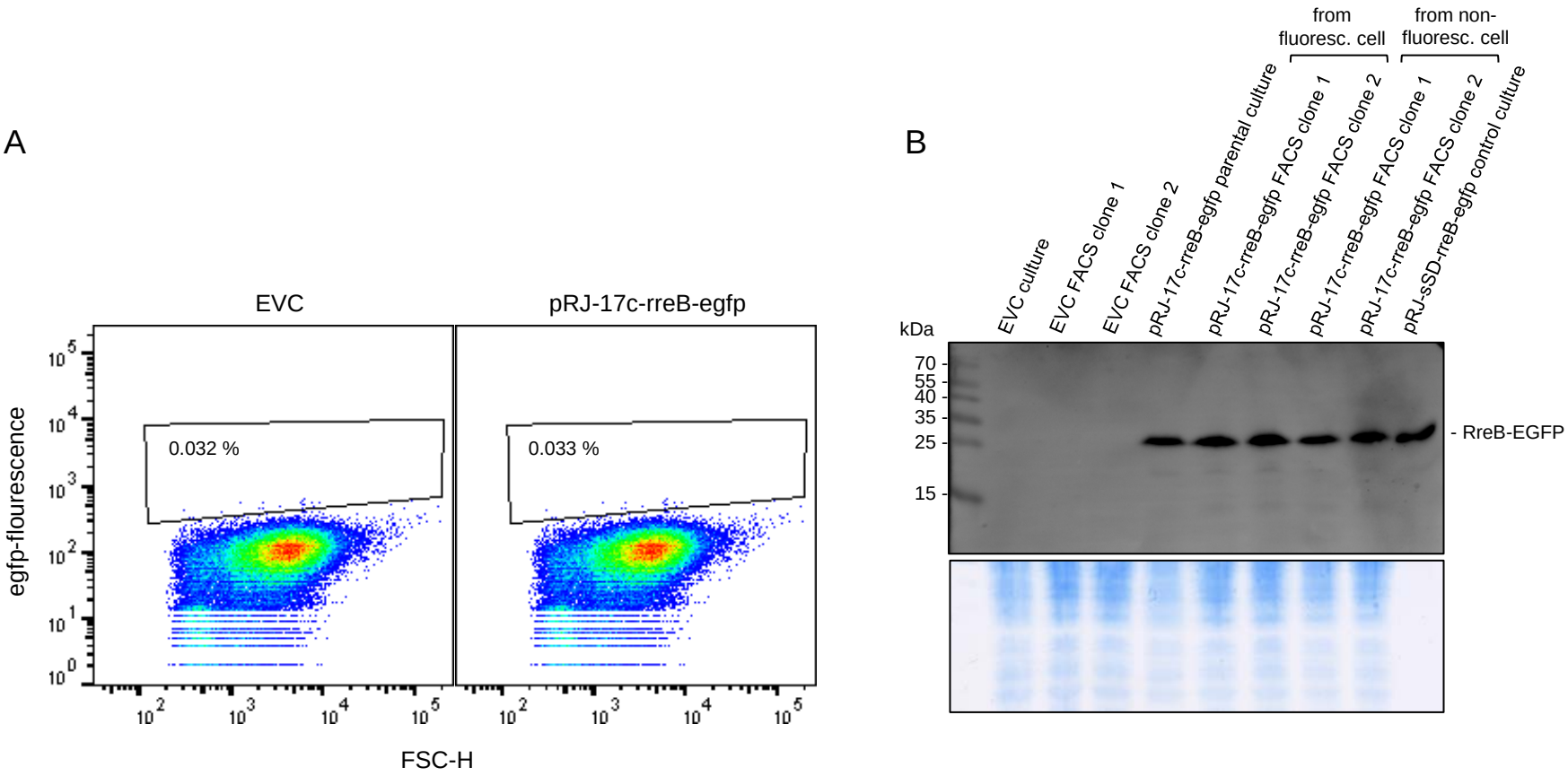

Figure S8. Flow cytometry and FACS analysis of *B. japonicum*. A) Flow cytometry analysis of *B. japonicum* populations with pRJPaph-MCS (empty vector control, (EVC)) or pRJ-17c-rreB-egfp, as indicated above the panels. Density plots of EGFP fluorescence versus FSC revealed no significant cell-to-cell variability regarding the fluorescent output within the two population. The percentage of fluorescent cells (P1) is given**. B)** FACS was used to obtain single-cell originating cultures for Western blot analysis with GFP-specific antibodies. A culture containing pRJ-sSD-rreB-egfp was used as a positive control; in this case 30-fold less cells were used. The bottom panel shows a Coomassie Blue stained SDS-polyacrylamide gel after electrophoresis visualizing the loaded protein amounts. Migration of marker proteins (M) in the gel is indicated at the left side in kDa.

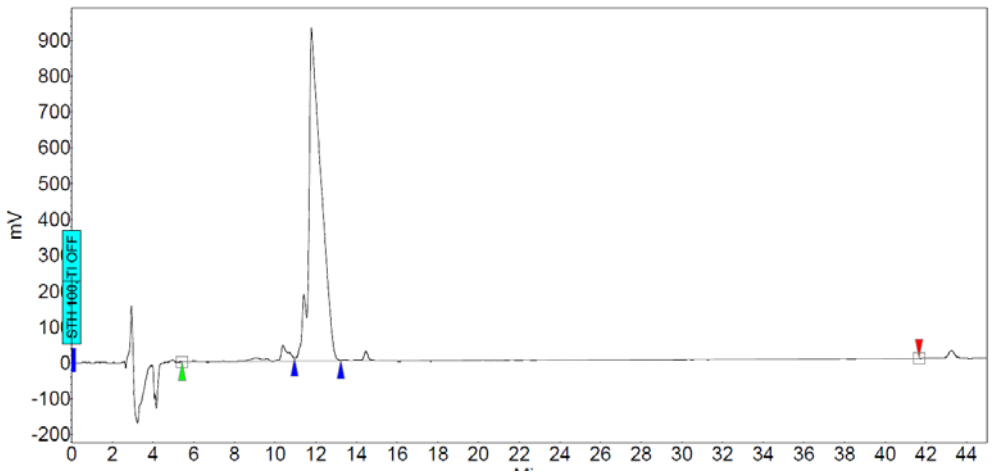

Figure S9: analytical HPLC-chromatogram of the purified RreR. The purity was > 90%.

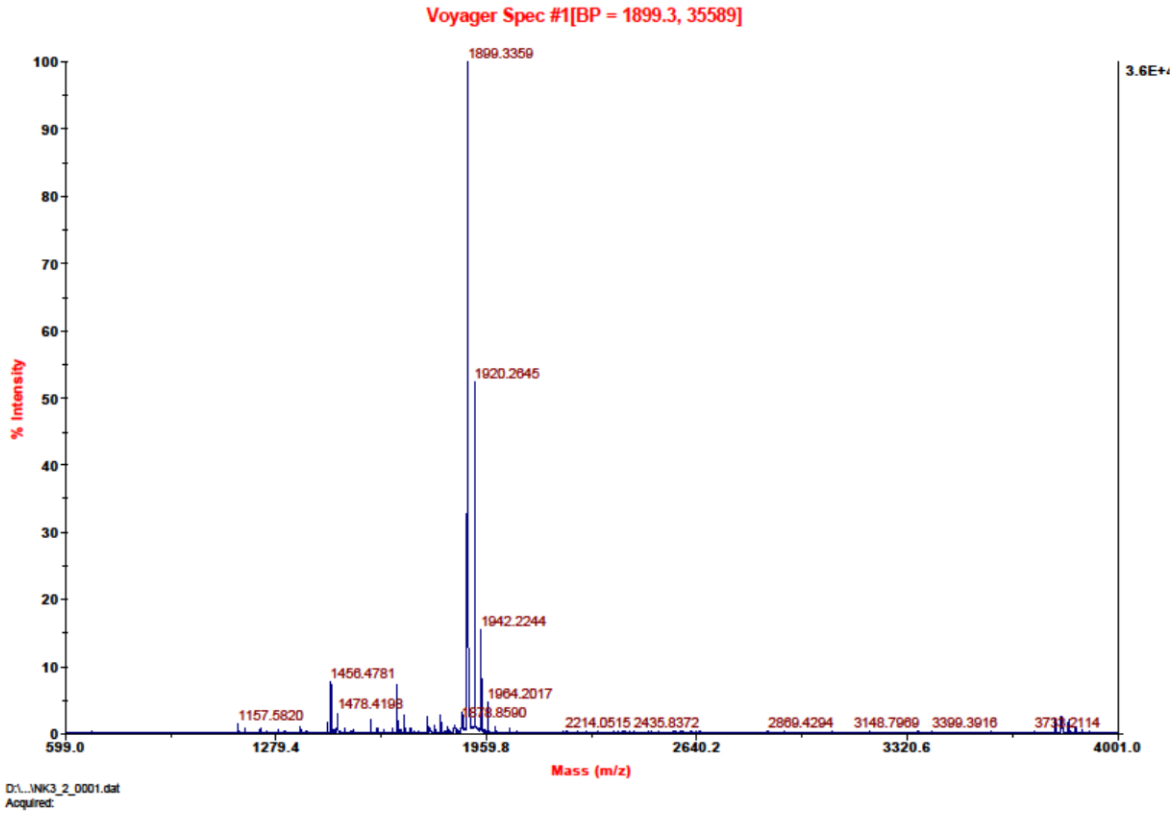

Figure S10: Matrix-assisted laser desorption/Ionization (MALDI) mass analysis of the purified RreR.

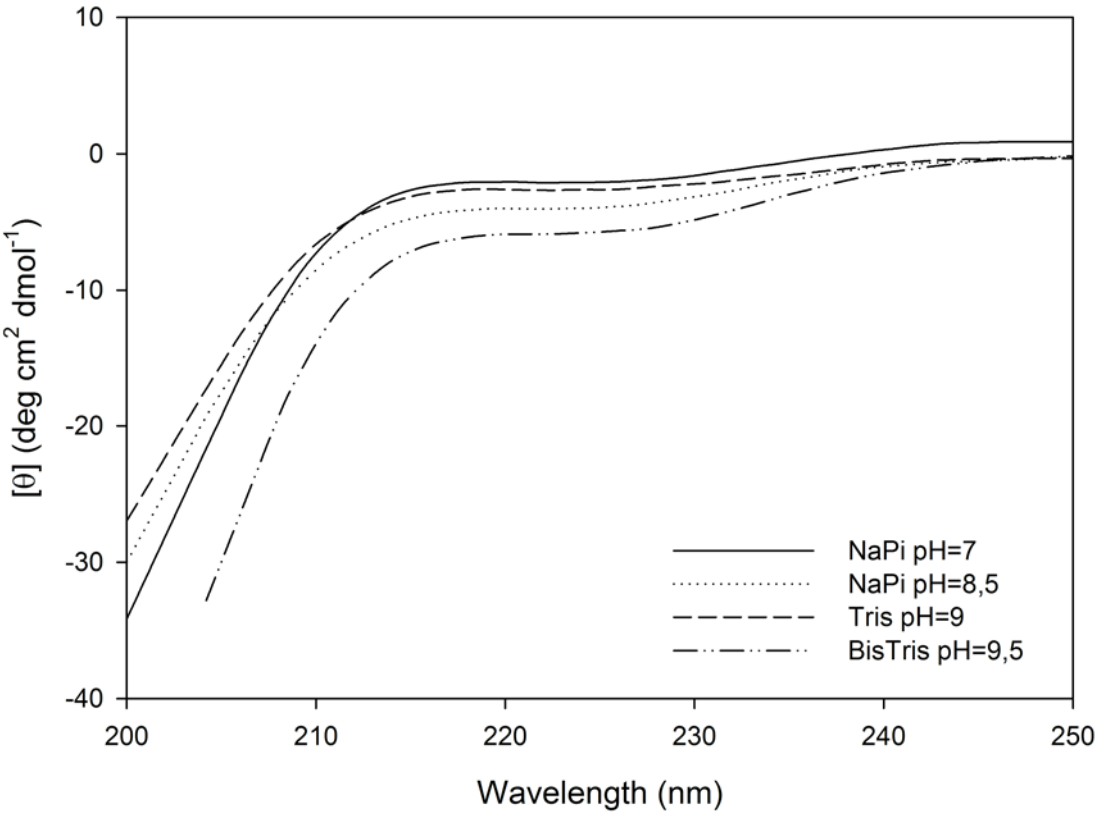

Figure S11: CD-spectra of RreR in different buffers.

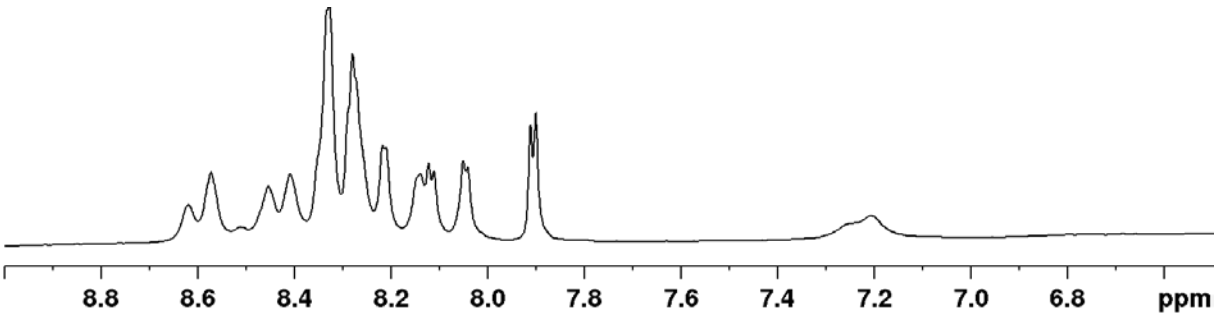

Figure S12: 1D ^{1}H-NMR-spectra of the amide, amino and aromatic proton resonances of RreR.